Energy partitioning in the femtosecond-laser-induced associative D_2 desorption from Ru(0001)

Steffen Wagner, Christian Frischkorn,* and Martin Wolf
Fachbereich Physik, Freie Universität Berlin, Arnimallee 14, 14195 Berlin, Germany

Marco Rutkowski and Helmut Zacharias
Physikalisches Institut, Westfälische Wilhelms-Universität, Wilhelm-Klemm-Straße 10, 48161 Münster, Germany

Alan C. Luntz
Fysisk Institut, Syddansk Universitet: Odense, Campusvej 55, 5230 Odense M, Denmark
(Received 15 July 2005; revised manuscript received 14 September 2005; published 3 November 2005)

Energy transfer to different degrees of freedom during the femtosecond-laser-induced recombinative desorption of D_2 from a deuterium-covered Ru(0001) surface ($D_{ads}+D_{ads}/Ru \rightarrow D_{2,gas}+Ru$) has been investigated. $(1+1')$-resonance-enhanced multiphoton photoionization (REMPI) and time-of-flight (TOF) measurements are utilized to provide information on the internal and external (translational) energy content, respectively. Rovibrational population distributions of the reaction product are detected via various $B\,^1\Sigma_u^+ \leftarrow X\,^1\Sigma_g^+$ Lyman bands using tunable vacuum ultraviolet laser radiation in the resonant excitation step. Rotational quantum state populations in the vibrational ground state and the first excited state are measured yielding average rotational energies of $\langle E_{rot}\rangle/k_B = 800$ and 1500 K, respectively, for an absorbed laser fluence $\langle F\rangle$ of 85 J/m^2. In addition, a mean vibrational energy of the desorbing molecules is extracted which amounts to $\langle E_{vib}\rangle/k_B = 1200$ K. Extensive TOF measurements enable complete energy balancing with $\langle E_{trans}\rangle/2k_B = 2500$ K at $\langle F\rangle = 85$ J/m^2 and underline the nonthermal and unequal energy partitioning between the different degrees of freedom within the reaction product. The effects of multidimensional electronic friction between substrate and adsorbate layer and peculiarities of the potential energy landscape governing the D_2 recombination are discussed.

DOI: 10.1103/PhysRevB.72.205404 PACS number(s): 68.43.Tj, 82.53.−k, 82.20.Kh, 33.80.Rv

I. INTRODUCTION

For a microscopic understanding of chemical reactions at surfaces (e.g., in heterogeneous catalysis), it is essential to obtain detailed knowledge on the underlying elementary processes. The reaction mechanism, the pathways and time scales of energy flow and the energy partitioning between different degrees of freedom of the reaction products are of key interest. Potential energy surfaces (PESs) are typically used to describe the nuclear motion of the interacting molecules or atoms en route from the educt to the product state. Thus, it has been a challenging task for theory to calculate a sufficiently accurate PES landscape to explain experimentally observed phenomena and for the experiment to provide observables which serve as benchmarks to check the current knowledge on the reaction system.[1–7]

Chemical reactions initiated by absorption of ultrafast, i.e., femtosecond (fs), light pulses have been the center of interest in recent years due to their intrinsic capability to characterize and trace the system on atomically relevant time scales.[8] At surfaces, it has become possible to distinguish physically different reaction scenarios like phonon-mediated from electron-mediated reaction pathways.[9,10] Among several investigated systems (e.g., NO, CO, CO+O, H_2),[9–16] the recombination of two atomically bound hydrogen atoms on a Ru(0001) surface, which form a H_2 molecule and leave the metal substrate, acts as a prototype of a fs-laser-induced surface reaction due to its structural simplicity and the fact that detailed information on this system has been already achieved.[10,11,17] An ultrafast time scale of energy transfer from the substrate to the adsorbate, a nonlinear reaction yield dependence on the applied laser fluence, together with a remarkably strong isotope effect have been found, all of them indicating a hot substrate electron-driven reaction mechanism. Peculiarities like a threshold-like coverage dependence of the desorption yield[11] and promotion effects in isotopically substituted surroundings of the reactants[10] have also contributed to a quite detailed picture of the associative hydrogen desorption from ruthenium. However, only little is known about the energy partitioning during the reaction. Earlier time-of-flight (TOF) measurements showed that the fs-laser-induced reaction releases the nascent H_2 molecules from the surface with very high translational energy.[10] The energy content in internal degrees of freedom (vibrational and rotational) still remained unknown.

Investigations on the energy partitioning between different degrees of freedom of the reaction product in a surface reaction offer additional insights into the underlying mechanism. Under excitation conditions of thermal equilibrium, e.g., in temperature-programmed desorption or nanosecond-laser pulse excitation, *nonactivated* reaction systems[18,19] [e.g., H_2+Pd(100)] typically show an equally balanced energy partitioning, while the reaction proceeds adiabatically on the electronic ground state. In contrast, *activated* systems[20–22] [e.g., H_2+Cu(100) or Cu(111)] typically exhibit an energy content of the reaction product which is unequally distributed between the different degrees of freedom. Depending on the location of a reaction barrier in the entry or exit channel (referred to as "early" and "late" barrier, respectively) of the electronic ground state, translational or vibrational excitation may facilitate the reactants to overcome the transition state (TS).[23] The topology of the PES also deter-

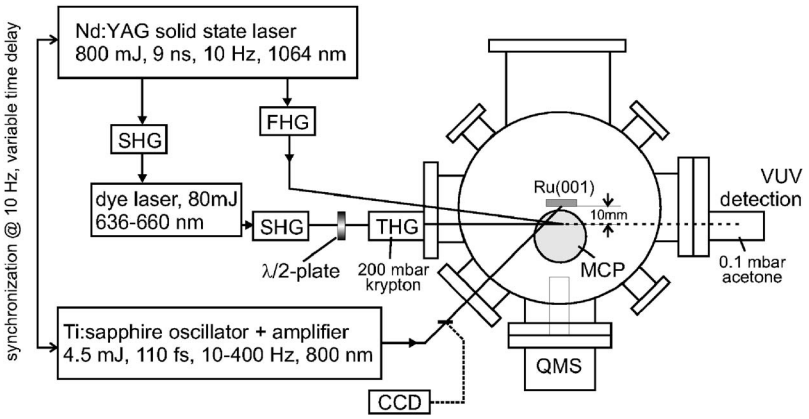

FIG. 1. Schematic diagram of the experimental setup combining a high-power femtosecond-laser system with tunable narrow-bandwidth vuv generation based on a solid-state laser-pumped dye laser. (SHG, THG, and FHG indicate second, third, and fourth harmonic generation, respectively.) Experiments are performed under ultrahigh vacuum conditions, where the D_2 molecules are formed and analyzed after desorption from the Ru surface.

mines to which extent in a recombinative desorption reaction the initial excitation normal to the surface at an early stage of the reaction might be converted to lateral and ultimately to interatomic motion, i.e., vibration.

Nonadiabatic effects, however, can also result in an unequal energy transfer into different degrees of freedom of the reaction product as seen in the associative desorption of N_2 from Ru(0001).[24] In these studies, contrary to expectations, the nascent N_2 molecules carry only little vibrational energy. Apparently, they lose most of their energy on their way beyond the reaction barrier which was explained by strong nonadiabatic coupling of the vibrational coordinate to electron-hole pairs. Up to now, only few examples of nonequilibrium (fs-laser) excitation experiments in conjunction with measurements of final-state energy distributions exist. So far, these studies have exclusively focused on the desorption of molecularly adsorbed diatomic species like NO from Pd, Pt or NiO and CO from Cu, respectively.[12–16] For example, in studies on the NO desorption from a Pd(111) surface induced by fs-laser pulses, markedly nonthermal rotational and vibrational distributions were found for the desorbing molecules underlining that a different reaction mechanism is operative than in thermal equilibrium.[12]

In this paper, we report on extensive TOF measurements as well as on state-selective investigations of desorbing D_2 molecules from a Ru(0001) surface originating from the hot-electron mediated $D+D \rightarrow D_2$ reaction. While in previous experiments TOF data were only recorded for a single laser fluence,[10] we have now obtained spectra over a wide fluence range, which show a significant dependence of the translational energy on this experimental parameter. They also reveal a clear isotope effect in the translational energy between H_2 and D_2 molecules, which was not observed in the early experiments. In addition, we find that both the fluence dependence and the isotope effect are qualitatively reproduced by employing the two-temperature and the electronic friction model (see below) used to describe the energy transfer processes after fs-laser excitation of a metal substrate. Moreover, our resonance-enhanced multiphoton photoionization (REMPI) data of the D_2 product demonstrate that the excess energy is distributed unequally between external and internal and also within internal degrees of freedom. Translational excitation is found to be more than five (four) times higher than the rotational (vibrational) contribution. In addition, the vibrational ground state exhibits a non-Boltzmann-like occupation distribution in the rotational degree of freedom with a distinct overpopulation of low J states. Remarkably, in establishing an energy balance based on the averaged energies, our frictional modeling again successfully describes the D_2/Ru(0001) system. Finally, we observe a clear molecular alignment due to which the desorbing D_2 molecules predominantly leave the surface in a helicopterlike motion. All these experimental findings are discussed in terms of the current level of theoretical modeling of nonadiabatic energy transfer processes underlying the associative D_2 desorption after fs-laser excitation.

II. EXPERIMENT

The experimental setup is shown in Fig. 1. It comprises a high-power femtosecond (fs) laser, a tunable narrow-bandwidth nanosecond (ns) vacuum ultraviolet (vuv) laser source, and an ultrahigh vacuum (UHV) chamber with a base pressure of less than 1×10^{-10} mbar. The single-crystalline Ru(0001) sample is mounted on a liquid nitrogen cryostat which in combination with resistive heating allows temperature control between 90 and 1530 K. Besides standard surface science tools for preparation and analysis of a well-defined D/Ru(0001) system, a quadrupole mass spectrometer (QMS), and an ion detector are employed for detection of the D_2 reaction yield and the respective ions. A saturation coverage [1 monolayer (ML)] of deuterium with D-(1×1) structure is achieved by heating the Ru crystal to 1530 K and subsequent dosing of 50 L D_2 at 170 K.[11,25] After preparation, the fs-laser-induced D_2 recombination experiments are performed at a sample temperature of 100 K.

The ultrashort light pulses of 130 fs duration at 800 nm center wavelength are generated in an amplified Ti:sapphire-based fs-laser system with pulse energies up to 4.5 mJ at 400 Hz.[11,26] For recording the time-of-flight spectra of the desorbing D_2 molecules, the D-covered Ru surface is irradiated with an unfocused beam (diameter 5 mm) of the fs laser under an angle of incidence of 45°. The time-of-arrival distributions of the desorbing particles are detected by a QMS whose distance to the crystal surface can be varied from

16 to 19 cm. A low repetition rate of 20 Hz set by a pulse picker together with an optical shutter enables us to record the TOF spectrum of each single laser pulse separately. The flight distances by a factor of 3 to 4 larger with respect to previous experiments[10] allow for a more accurate measurement of the translational excess energy, since the comparatively fast hydrogen molecules (typical velocities ~5000 m/s and higher) disperse temporally more in the newer setup. Thus, the time resolution due to the discretized detector channels is significantly enhanced. In addition, the obtained TOF spectra are corrected for the ion flight time inside the QMS in a more reliable way by comparing TOF spectra at different, but known flight distances between the Ru sample and the QMS ionizer.

The vuv laser source[27] is based on a neodymium-doped yttrium aluminum garnet (Nd:YAG) laser pumped dye laser whose second harmonic is frequency tripled in a krypton cell. Tunable vuv laser radiation is obtained in the $\lambda = 106-110$ nm spectral range, which serves in the resonant excitation step of the $(1+1')$ REMPI process. For normalization reasons, the vuv intensity is recorded for each single laser pulse via the ion signal produced in an acetone-filled monitor cell, which is attached to the exit window of the UHV chamber. In addition, an unused portion of the fundamental output of Nd:YAG laser is quadrupled which yields uv photons at $\lambda = 266$ nm and is used for the nonresonant ionization of the excited D_2 species.

Employing the REMPI technique in the state-selective measurements of the fs-laser-induced D_2 molecules, both laser systems (fs and vuv) are synchronized at 10 Hz. The focussed beam (diameter 0.5 mm) of the fs laser is scanned over the deuterium-covered ruthenium surface by moving the crystal via computer-controlled stepper motors. In order to detect the desorbing D_2 molecules, the uv and vuv laser beams are brought in overlap under an angle of 12° in a plane parallel to the crystal surface at a focus 10 mm in front of the crystal. The temporal delay between the fs and the vuv laser is adjusted so that only molecules at the maximum of the TOF spectrum are ionized. This guarantees that a molecular subensemble of almost identical velocity is probed. The deuterium molecules are electronically excited by the vuv radiation in the $B\,^1\Sigma_u^+(v',J') \leftarrow X\,^1\Sigma_g^+(v'',J'')$ Lyman system. In a second step, the uv photons ionize the excited D_2 molecules which are then detected by microchannel plates (MCPs) mounted underneath the Ru crystal in a lower plane of the UHV chamber. In addition, by changing the polarization of the excitation photons via a half wave plate before the tripling unit, the rotational quadrupole alignment $A_0^{(2)}$ of the desorbing D_2 molecules can be determined.[27]

III. RESULTS

This section will be divided into two parts; the first concerns the translational degree of freedom which we address with *non*-state-selective time-of-flight measurements, while the second comprises state-selective experiments with REMPI detection yielding information on the internal degrees of freedom like rovibrational population distributions and rotational alignment.

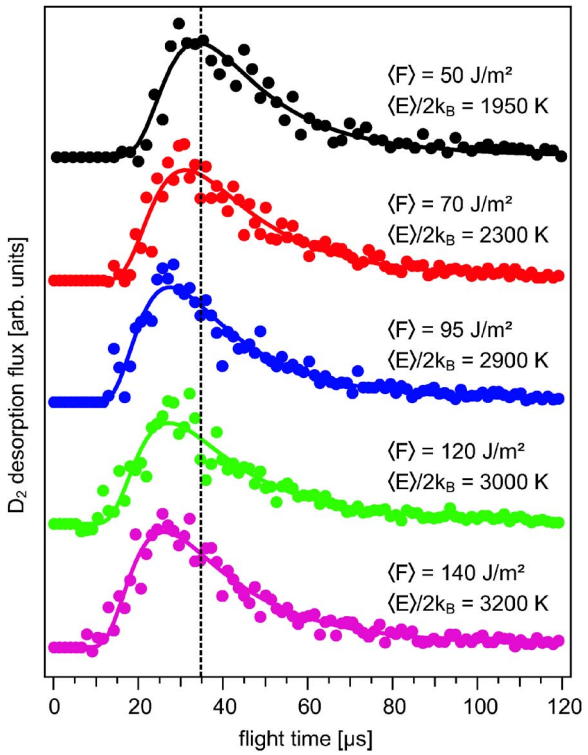

FIG. 2. (Color online) TOF distributions of fs-laser-induced D_2 for various laser fluences $\langle F \rangle$ ranging from 50 to 140 J/m^2. Modified Maxwell-Boltzmann distributions (solid lines) fit the experimental spectra. Mean translational energies expressed in kelvin are obtained from the second moments of the discrete experimental data points. Note the clear shift to shorter flight times, i.e., higher translational energies, with increasing laser fluence.

A. Time-of-flight measurements

Figure 2 presents TOF spectra of desorbing D_2 molecules induced by fs-laser excitation for various laser fluences ranging from 50 to 140 J/m^2. Each TOF data set is well reproduced by a single modified Maxwell-Boltzmann distribution.[28] This suggests that only one reaction channel dominates the recombination process. The mean translational energy of the desorbing particle flux is derived from the second moment of the discrete data points and may be assigned to a translational temperature according to $T_{\mathrm{trans}} = \langle E_{\mathrm{trans}} \rangle / 2k_{\mathrm{B}}$.[29–32] The translational temperatures obtained range from 2000 to 3200 K with error margins of ±200 K. With increasing laser fluence, a clear shift to shorter flight time, i.e., higher T_{trans}, is observed (see Fig. 3). In these experiments, all fluences $\langle F \rangle$ are given as *absorbed* yield-weighted fluences which account for both the energy deposited into the system and the non-uniform energy distribution across the spatial profile of the laser beam.[11,13,26] The latter is important, since due to the highly nonlinear fluence dependence of the reaction yield areas of the beam profile with higher intensity contribute to the overall yield to a much greater extent than less intense sections do.[11]

In Fig. 3, the mean translational energies $\langle E_{\mathrm{trans}} \rangle / 2k_{\mathrm{B}}$ of D_2 and H_2 leaving the Ru surface after fs-laser excitation are plotted as a function of $\langle F \rangle$. Within the fluence range applied

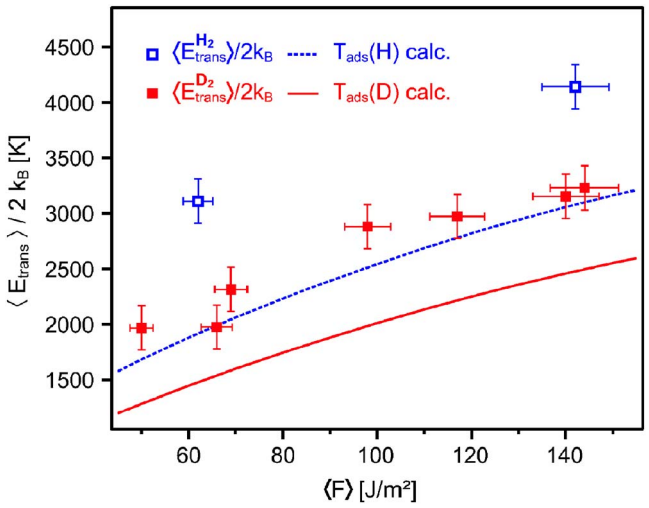

FIG. 3. (Color online) Translational energies $\langle E_{\mathrm{trans}}\rangle/2k_{\mathrm{B}}$ of D_2 and H_2 desorbing from Ru(0001) after fs-laser excitation as a function of the yield-weighted laser fluence $\langle F\rangle$. Solid and dashed lines show the yield-weighted adsorbate temperature for a D and H layer, respectively (see text). Both experiment and model show a clear isotope effect. The mean translational energies expressed in kelvin are by a factor of ~1.35 larger than the calculated yield-weighted adsorbate temperature values. Note extrapolation of a linear fit to experimental D_2 data results in an intercept of the $\langle E_{\mathrm{trans}}\rangle/2k_{\mathrm{B}}$ axis at 1250 K.

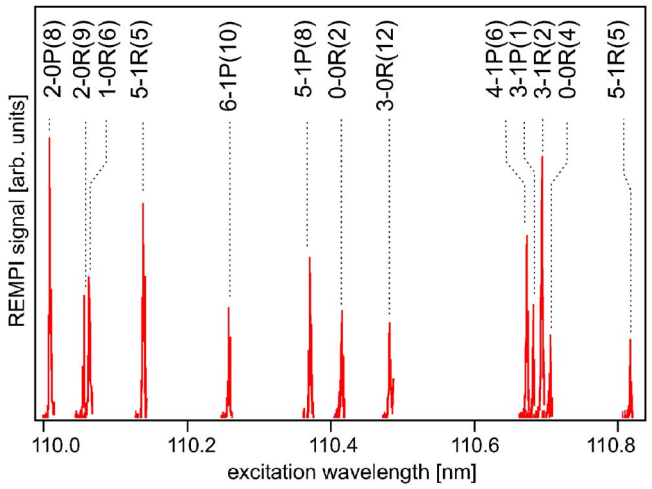

FIG. 4. (Color online) Ionization spectrum of D_2 desorbing from D/Ru(0001) after fs-laser irradiation with $\langle F\rangle$=85 J/m^2 versus the vuv wavelength of the REMPI excitation step. The line notation of the resonances is explained in Ref. 35.

in our experiment, $\langle E_{\mathrm{trans}}\rangle/2k_{\mathrm{B}}$ increases by more than 60% with increasing fluence. This graph also reveals a pronounced isotope effect in the translational energies between desorbing H_2 and D_2 molecules. The $\langle E_{\mathrm{trans}}\rangle/2k_{\mathrm{B}}$ values for H_2 and D_2 differ by ~1000 K with the higher energies for the lighter isotope. It is noteworthy that both the fluence dependence and the isotope effect in the translational excess energy of the reaction product have not been observed in previous measurements due to the limited resolution of the earlier TOF spectra.[10]

In order to compare these translational energies with results from theoretical modeling of energy flow between the laser-excited substrate and the adsorbate layer, a yield-weighted adsorbate temperature is introduced. These calculations are based on the two-temperature model[33] used for the Ru substrate in conjunction with adsorbate-mass-dependent electronic friction for the substrate-adsorbate interaction.[34] Details of this modeling have been reported previously;[11,26] however, fundamental aspects relevant to the results of this paper will be given further below in the discussion section. With the time profiles of the adsorbate temperature and the reaction yield, we determine an averaged temperature for the adsorbate heat bath by weighting the transient $T_{\mathrm{ads}}(t)$ with the respective reaction rate $R(t)$. The solid and dashed lines in Fig. 3 mark the outcome of this weighting method for both isotopes H_2 and D_2. The general trends in the fluence dependence and the isotope effect are well reproduced, albeit the absolute values of the yield-weighted adsorbate temperature are by a factor of 1.35 smaller than the experimental $\langle E_{\mathrm{trans}}\rangle/2k_{\mathrm{B}}$. In addition, to obtain the minimum energy released into the translational degree of freedom, we extrapolate the $\langle E_{\mathrm{trans}}\rangle/2k_{\mathrm{B}}$ data to zero fluence and find an axis intercept of 1250 K (~100 meV) for D_2 by a linear fit. In this way, contributions to $\langle E_{\mathrm{trans}}\rangle$ from the laser excitation and from the ground state barrier can be separated. As will be discussed below, the obtained value of 100 meV represents an upper bound for the D_2 recombination barrier.

B. Rovibrational state distribution and alignment

Figure 4 shows the REMPI ion signal of desorbing D_2 molecules after fs-laser irradiation of the D-covered Ru(0001) surface with an absorbed laser fluence of 85 J/m^2. Here, resonances of various rovibrational states in the Lyman (0-0) to (3-0) and (3-1) to (5-1) bands detected in the experiment are plotted versus the vuv excitation wavelength.[35] With known transition probabilities for both the excitation and the ionization step, the rovibrational state population $N(v'',J'')$ is derived from the vuv-intensity normalized REMPI signal I according to

$$N(v'',J'') \propto I/[|R_e^{n'n''}|^2|R_{\mathrm{vib}}^{v'v''}|^2 S_{J'J''}K(v',J')\chi]. \qquad (1)$$

$|R_e^{n'n''}|^2$ and $|R_{\mathrm{vib}}^{v'v''}|^2$ denote the electronic transition moment and the vibrational wave function overlap, i.e., the Franck-Condon factor, respectively. $S_{J'J''}$ stands for the Hönl-London factor which determines the angular momentum part of the overall transition probability. $K(v',J')$ takes the relative detection sensitivity of the resonant intermediate state into account and was determined in previous experiments.[27,36] The influence of the rotational alignment of desorbing molecules is included by the polarization factor χ=f(v'',J''). This factor compensates for the dependence of the excitation probability on the angle between the transition moment and the polarization of the exciting vuv laser field. However, since we do not observe a dependence of the alignment on the rotational quantum number (see below), this

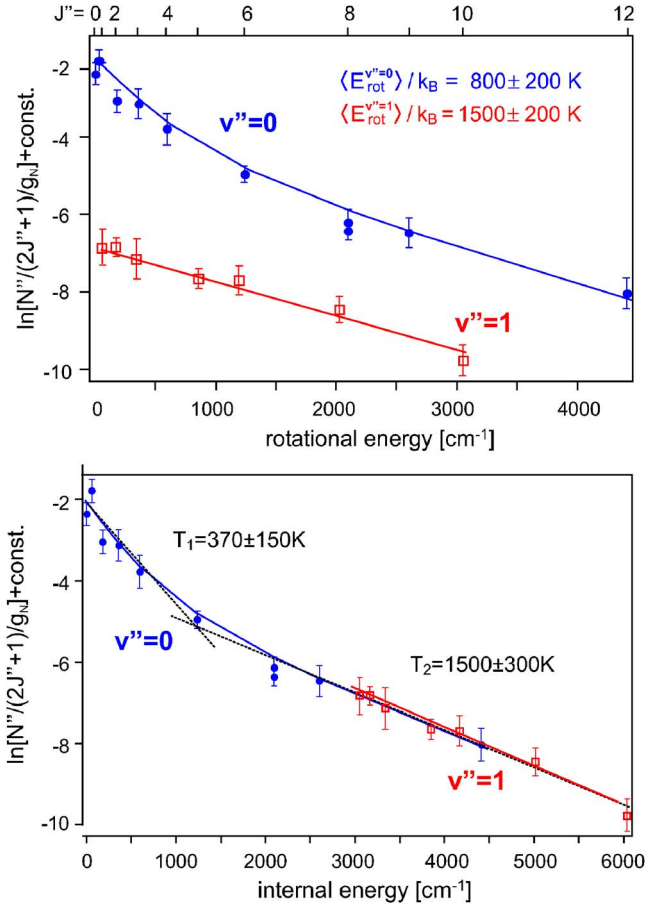

FIG. 5. (Color online) Rovibrational population distributions $N(v'',J'')$ of D_2 desorbing from Ru(0001) after fs-laser irradiation ($\langle F\rangle$=85 J/m^2). Boltzmann plots for the vibrational ground and first excited state are shown versus the rotational energy (top panel) and the total internal energy $E_{\mathrm{rot}}+E_{\mathrm{vib}}$ (bottom panel), respectively. Filled circles, $D_2(v''=0)$; open squares, $D_2(v''=1)$.

factor χ is set to 1 in the analysis of the state populations.

For further analysis, the obtained rotational state populations of the desorbing D_2 molecules are normalized by the statistical weight $(2J''+1)g_n$ with g_n allowing for the different multiplicity of ortho- versus para-type D_2. In Fig. 5, these normalized populations of the vibrational ground ($v''=0$) and first excited ($v''=1$) state are then averaged over P- and R-branch measurements and displayed in a semilogarithmic plot as a function of the rotational and the total internal energy, respectively. For a molecular ensemble in thermal equilibrium, such a Boltzmann plot of the rovibrational population distribution exhibits a linear slope which is inversely proportional to the rotational temperature T_{rot}. However, as evident in the upper panel of Fig. 5, the rotational population of the fs-laser-induced D_2 molecules in $v''=0$ clearly deviates from such a thermalized Boltzmann distribution. States with $J''<6$ show a distinct higher occupation. However, one can still calculate the respective mean rotational energy in the $v''=0$ state which amounts to $\langle E_{\mathrm{rot}}^{v''=0}\rangle/k_{\mathrm{B}}=800$ K. In contrast, in the first vibrationally excited state, the rotational population obeys a Boltzmann distribution and hence can be assigned formally to a rotational temperature of $T_{\mathrm{rot}}=\langle E_{\mathrm{rot}}^{v''=1}\rangle/k_{\mathrm{B}}=1500$ K.

If the rotational population distribution is plotted versus the total internal energy $E_{\mathrm{rot}}+E_{\mathrm{vib}}$, as done in Fig. 5 (lower panel), no vertical offset between the $v''=0$ and $v''=1$ state is seen. In addition, in the energy range where both vibrational states overlap, $v''=0$ states with $J''\geqslant 6$ share the same linear slope as rotational states in $v''=1$ do. Therefore, no preference of energy coupling into one or the other vibrational state can be asserted. Over the entire range of total internal energy, the measured rotational population distribution is reproduced best by a sum of two Boltzmann fits with temperatures $T_1=370$ K and $T_2=1500$ K. This again underlines the non-equilibrium conditions governing the D_2 desorption reaction.[10,11] Weighting those two Boltzmann distributions with the population of each rotational state in $v''=0$ and $v''=1$ results in an averaged rotational energy (in kelvin) of $\langle E_{\mathrm{rot}}\rangle/k_{\mathrm{B}}=910\pm200$ K. To complete the information on energy partitioning into the different degrees of freedom, the vibrational contribution is obtained by assuming a Boltzmann distribution between the $v''=0$ and $v''=1$ state. In this way, a vibrational temperature of $T_{\mathrm{vib}}=\langle E_{\mathrm{vib}}\rangle/k_{\mathrm{B}}=1200\pm250$ K is derived for the desorbing particle flux. D_2 molecules in the $v''=2$ or higher vibrational states could not be detected.

In addition, we have investigated the rotational alignment of the desorbing molecules. The nascent D_2 molecules are excited by vuv radiation with the polarization parallel and perpendicular to the surface normal axis. The ionization step has been saturated for both polarizations. The corresponding ion signal $I_{\parallel}$ and $I_{\perp}$ define the molecular polarization P with $P=(I_{\parallel}-I_{\perp})/(I_{\parallel}+I_{\perp})$. With this, the rotational alignment $A_0^{(2)}$ can be derived for the P and R branch by the following equations,[37]

$$A_0^{(2)}=\frac{-4P(2J''-1)}{(J''+1)(3-P)} \quad (P \text{ branch}) \tag{2}$$

and

$$A_0^{(2)}=\frac{-4P(2J''+3)}{J''(3-P)} \quad (R \text{ branch}). \tag{3}$$

Our results of the rotational alignment for several rovibrational states and laser fluences reveal neither a dependence on the quantum state nor a fluence dependence. However, a significant positive alignment was found exemplified for the 2-0P(8) transition with $A_0^{(2)}=0.27\pm0.15$. This value implies that about three- quarters, (74±6)%, of the molecules desorb with $|M_{J''}|\geqslant J''/2$, i.e., in a more helicopterlike rotation, and one- quarter, (26±6)%, with $|M_{J''}|<J''/2$, which corresponds a cartwheel-like motion.

As a final aspect before entering the discussion section, we address possible distortions of the nascent rovibrational population distribution and the respective molecular alignment of the desorbing D_2 molecules. Gas phase collisions immediately after desorption and prior to ionization may lead to a decay of both the population distribution (i.e., thermalization within the same and between different degrees of

freedom) and the rotational alignment (i.e., orientational randomization). For hydrogen molecules (H_2 and D_2), typical collision numbers for significant rotational energy transfer and vibrational relaxation are several hundred (100 to 1000) and several ten thousand (10^4 to 10^5) collisions, respectively.[38–40]

In our experiments, however, we estimate an average number of collisions per D_2 molecule during the flight to the detection volume of significantly less than 10. This value is based on depletion experiments, in which the desorption yield is detected as a function of the shot number of the laser impinging the same spot on the sample. The resulting maximum D_2 flux of $\sim 4\times 10^{13}/\mathrm{cm}^2$ is comparable to that in experiments with NO molecules desorbing from a LiF(100) surface.[41] In the latter case for NO, which has a similar collisional cross section as D_2,[41,42] a collisional number of only ~ 2 was found for three orders of magnitude in desorption times ranging from 3.5 ps to 1 ns. Our reasoning that gas phase collisions in the desorbing D_2 particle flux after desorption from the surface should not significantly distort neither the nascent rovibrational population distributions nor the initial rotational alignment is also supported by several experimental facts: We observe an overpopulation of low J'' numbers in $v''=0$, i.e., incomplete rotational thermalization together with a nonzero alignment,[43] and in the TOF spectra shown in Fig. 2, we find no evidence of a nozzling effect, i.e., narrowing of the velocity distributions with increasing laser fluence.[44]

IV. DISCUSSION

In order to establish an energy balance between the energy deposited into the metal substrate by the laser pulse and the energy content of the reaction product in the different degrees of freedom, we first recall the theoretical models typically used to characterize the energy transfer processes initiated by fs-laser excitation. The two-temperature model[33] describes the energy flow within the substrate after photoexcitation by treating the electron and phonon subsystems of the metal as coupled heat baths. The subsequent energy transfer from the substrate to the adsorbate is accounted for by a frictional approach[45] in which both substrate subsystems are coupled to the relevant reaction coordinate of the adsorbate by a one-dimensional (1D) friction coefficient. In purely electron-mediated surface processes, the modified electronic friction model (also 1D) by Brandbyge *et al.*[34] has been frequently applied as also in the present case of the fs-laser-induced associative desorption of hydrogen from Ru(0001).[46] The basic concept of this friction model is illustrated in the inset of Fig. 6. As has been reported in previous publications,[10,11,17] measurements of the two-pulse yield correlation and the fluence dependence of both the reaction yield and the isotope effect show that all data are consistently fitted with a single parameter set comprising the frictional coefficients $\eta_{el}=1/180$ and $1/360\ \mathrm{fs}^{-1}$ for H_2 and D_2, respectively, and the activation energy $E_a=1.35$ eV. Utilizing these values, one obtains the time profiles of the electron, phonon and adsorbate temperature together with the D_2 reaction yield as displayed in Fig. 6 for an absorbed fluence

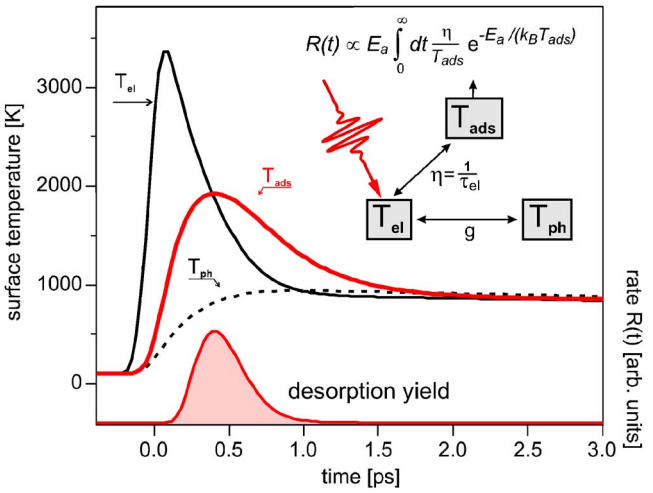

FIG. 6. (Color online) Time profiles of electronic and phononic temperatures T_{el} and T_{ph} of the Ru substrate together with the adsorbate temperature T_{ads} of a D adlayer and its respective reaction rate $R(t)$ after fs-laser excitation with $\langle F\rangle=85\ \mathrm{J/m}^2$. In the calculations based on the two-temperature (Ref. 33) and the modified electronic friction (Ref. 34) model, the previously obtained values for the electronic coupling time and the activation energy were used (Ref. 10). The basics of these models are illustrated in the inset.

$\langle F\rangle=85\ \mathrm{J/m}^2$. The T_{ads} transient follows the electronic temperature with a certain time delay and reaches its maximum at approximately 400 fs after the fs-light pulse strikes the Ru surface. To represent the adsorbate heat bath by a single average temperature, the already mentioned yield-weighted adsorbate temperature $T_{ads}^{YW}=\int_0^\infty T_{ads}(t)R(t)dt/(\int_0^\infty R(t)dt)$ is used. As visualized in Fig. 6, $T_{ads}(t)$ at time t contributes to T_{ads}^{YW} according to its respective reaction rate $R(t)$. For a fluence of $85\ \mathrm{J/m}^2$ applied in our experiments with the state-selective REMPI detection, a $T_{ads}^{YW}=1800$ K is obtained.

Besides this yield-weighted adsorbate temperature, all energies and temperatures derived for internal and external degrees of freedom in the desorbing D_2 flux are summarized in Table I. One can now determine the entire energy content of the particle flux along the surface normal according to[47]

TABLE I. Summary of energy partitioning between different degrees of freedom in the fs-laser-induced D_2 recombination. Temperatures are derived from $\langle E_{vib,rot}\rangle/k_B$ for vibrational and rotational contributions, respectively, and $\langle E_{trans}\rangle/2k_B$ for the translational degree of freedom. The yield-weighted (YW) adsorbate temperature T_{ads}^{YW} is obtained from a respective weighting procedure of the calculated time profiles out of two-temperature and friction model calculations (see text and Fig. 6).

	Energy (meV)	Temperature (K)
Translation	430	2500
Vibration	100	1200
Rotation	80	910
Modeled T_{ads}^{YW}	155	1800

$$\langle E_{\mathrm{flux}}\rangle = \langle E_{\mathrm{trans}}\rangle + \langle E_{\mathrm{vib}}\rangle + \langle E_{\mathrm{rot}}\rangle = 2k_{\mathrm{B}}T_{\mathrm{trans}} + k_{\mathrm{B}}T_{\mathrm{vib}} + k_{\mathrm{B}}T_{\mathrm{rot}}. \tag{4}$$

Under full thermal accommodation conditions between all degrees of freedom of the D_2 product molecules and the adsorbate layer, $E_{\mathrm{ads}}=4k_{\mathrm{B}}T_{\mathrm{ads}}^{\mathrm{expt}}$ would be obtained by virtue of Eq. (4) where $T_{\mathrm{ads}}^{\mathrm{expt}}$ describes a common adsorbate temperature. Assuming $E_{\mathrm{ads}}=\langle E_{\mathrm{flux}}\rangle$, we can now derive $T_{\mathrm{ads}}^{\mathrm{expt}}=\langle E_{\mathrm{flux}}\rangle/4k_{\mathrm{B}}$ and obtain with our experimental results for T_{trans}, T_{vib} and T_{rot} a value for $T_{\mathrm{ads}}^{\mathrm{expt}}$ of 1780 K which is in excellent agreement with the modeled yield-weighted adsorbate temperature $T_{\mathrm{ads}}^{\mathrm{YW}}$. Given that in the electronic friction model one assumes a time-independent and one-dimensional friction coefficient η together with a single adsorbate temperature T_{ads} which uniformly characterizes the adlayer, these matching temperatures appear rather astonishing. Note that the measurements of the external and internal energy content of the desorbing product molecules (i.e., the TOF spectra and rovibrational population data) were taken from a molecular ensemble which desorbs under normal direction. In the case of a significantly broad angular distribution of the desorbing particles, the energy balance performed here could fall short of the energy share transferred to D_2 molecules leaving the Ru surface under angles different from the normal direction. In reverse, however, since the models applied satisfactorily describe the energy balance, a rather peaked angular desorption distribution of the D_2 is supported which yet needs to be verified in additional experiments.

We now want to address the apparent unequal partitioning of excess energy between the different degrees of freedom of the D_2 product molecules. As seen in Table I, the energy transferred to translational, vibrational and rotational degrees of freedom scales as 5.4:1.3:1; the hydrogen recombination reaction initiated by fs-laser pulses releases the product molecules with a predominantly translational excitation. In contrast, non-activated reactions proceeding under full equilibrium conditions of the underlying substrate as in permeation experiments,[27,36] in which the reactants permeate through a single-crystal and recombine from its surface, show (almost) equal energy partitioning between the different degrees of freedom. Small deviations from complete energy accommodation are typically attributed to dynamical effects such as rotational cooling and/or vibrational heating.[27,36] The former is rationalized by steering forces acting during the adsorption process. Molecules in low rotational states are more readily steered into a favorable orientation through the PES landscape than species in high J states. Consequently, due to the principle of detailed balance, this results in a higher desorption probability for low J molecules. The latter effect, the vibrational heating in non- or only slightly activated systems, can be explained by the adiabatic lowering of vibrational frequencies upon dissociation.[48]

In hot-electron driven reactions, where desorption of a *molecular* adsorbate like NO or CO (contrary to the H_2 recombination of two hydrogen *atoms*) is initiated by fs-laser pulses, a pronounced vibrational excitation of the product is found.[12,13] In both cases, the NO desorption from Pd(111),[12] and CO from Cu(100),[13] the high vibrational energy content of the desorbing molecules was explained to be also of dynamical nature. The highly elevated vibrational temperature (up to $\geqslant$2000 K) reflects the high electronic temperature, since the intramolecular stretch vibration of these molecules remains rather undamped in the desorption exit channel. In addition, translational cooling might be observed, which means that due to the short interaction time during the desorption process the desorbing molecule leaves the surface without complete equilibration with the heat bath of the solid.[49]

Besides the topology of the electronic ground state on which the chemical reaction evolves and those dynamical effects which influence the product energy partitioning, also a multidimensional coupling between substrate and reactants as would be expressed in a multidimensional friction coefficient might cause a substantially unbalanced energy partitioning. The latter is based on the concept that energy does not flow along a single pathway but is transferred via different channels with distinct time constants. Recent *ab initio* calculations on the frictional coupling for H_2/Cu(111) and N_2/Ru(0001) indeed reveal anisotropic friction coefficients between the normal and the lateral adsorbate coordinate.[50] In these activated systems, the coupling near the adsorption minimum of the distance coordinate z (along the surface normal) to the electronic system of the metal substrate is found to be considerably larger than that of the interatomic separation coordinate $d_{X\text{-}X}$. In both cases, this implies an initially strong adsorbate-substrate vibration, whereas the lateral movement is less excited at the beginning of the recombination process.

First attempts to treat the hydrogen/Ru system have just started.[51–53] While Kroes, Baerends and coworkers[51,52] investigated the interaction of a single H_2 molecule with the bare Ru surface in a fully six-dimensional quantum dynamics approach, the work underway by Luntz[53] and coworkers aims more towards an understanding of the nonadiabatic multidimensional coupling between substrate and adsorbate and, moreover, incorporates a fully covered surface. All of these studies agree that a small barrier of 60 to 80 meV is located in the entry channel of the adsorption process. This barrier height is in good agreement with the extrapolated minimum translational energy obtained from our TOF results (see Fig. 3), (especially given the fact that the axis intercept was obtained by a linear instead of an apparently down-curved fit of the $\langle E_{\mathrm{trans}}\rangle/2k_{\mathrm{B}}$ versus $\langle F\rangle$ data). First results of frictional calculations indicate that in contrast to the above mentioned H_2/Cu(111) and N_2/Ru(0001) the recombining H atoms on Ru(0001) experience a rather isotropic coupling/friction at early stages of the reaction. However, close to the TS in the desorption exit channel, the friction coefficients explicitly differ in the z and d_{HH} coordinate with $\eta_z \approx 3\,\eta_{d_{\mathrm{HH}}}$.[53] Whether or not this explains the preferred translational excitation of the D_2 product in our experiment needs further clarification through dynamical trajectory simulations. For example, one intriguing question addresses the time window in which nonadiabatic electronic transitions occur after photoexcitation while the reactants move along the reaction path. Consequently, different sections of the PES landscape will influence the energy exchange between the Ru and the reactants differently and the frictional anisotropy near the TS of the

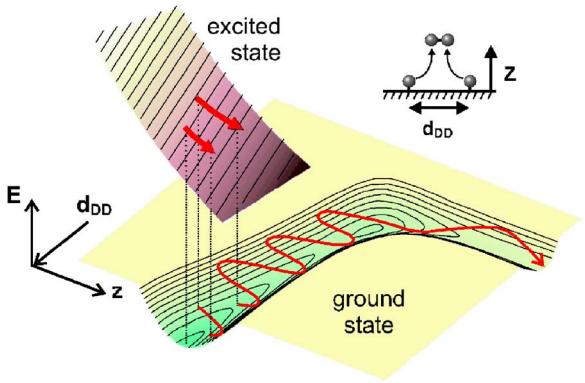

FIG. 7. (Color online) Illustration of the D_2 desorption process after fs-laser excitation. Coordinates denote the center-of-mass distance z of the D_2 molecule from the surface and the D-D interatomic distance d_{DD}. Note the qualitative character of the potential energy landscape and the exemplary trajectory demonstrating a possible route which results in predominantly translational energy and significantly less vibrational excitation. The ground PES is adopted from Ref. 52 in which the H_2 interaction with a clean Ru(0001) surface was calculated.

H_2/Ru(0001) might play an important role in the unequal energy partitioning observed in our experiments.

Finally, to illustrate the processes during the D_2 recombination, Fig. 7 sketches qualitative PESs involved in the reaction. According to the desorption induced by multiple electronic transitions picture,[54] the absorption of the fs-laser pulse initiates more than one electronic transitions between the ground and an electronically excited state. Figure 7 suggests one possible reaction scenario, in which an initially rather strong excitation of the z coordinate of the D atoms normal to the surface may lead to a predominantly translational excitation of the reaction product after turning around the elbow. However, steering effects and/or complex coupling between different degrees of freedom can cause additional complexity such that the visual illustration of the reaction in Fig. 7 might be too simplified. Note that the smaller rotational excitation with respect to the vibrational and translational energy release found in the desorbing D_2 molecules supports the reduced dimensionality of this representation $E=E(z,d_{DD})$, which is downsized from originally 6D to 2D. However, it is clear that only calculations which include *all* six dimensions will describe the D_2 desorption process appropriately with all experimental observations such as the reduced but not-vanishing rotational excitation, the observed non-Boltzmann-like rotational population[55] and the positive molecular alignment of the product molecules. In summary, based on the current level of knowledge without dynamical simulations, one cannot attribute the observed energy partitioning pattern solely to the dynamics on the ground state nor to the excitation process (multidimensional frictional coupling) unambiguously.

V. CONCLUSION

We have presented TOF and state-selective detection results on the fs-laser-induced D_2 recombination in order to address the energy partitioning between different degrees of freedom during reaction. The translational energy content was found to be crucially dependent on the absorbed laser fluence and the respective isotope H or D. This can be rationalized by the higher electronic temperature reached for the lighter isotope and for higher fluences. Measurements of the rovibrational population revealed that the D_2 molecules leave the Ru surface predominantly with high translational energy, low vibrational, and even less rotational excitation. The concept of frictional coupling with a single and time-independent coupling coefficient still describes the average energy $\langle E_{flux} \rangle$ of the desorbing D_2 astonishingly well, although it is incapable of accounting for the unequal distribution of energy between the different degrees of freedom of the reaction product. However, even within this 1D frictional model there are evidences that this simplifying assumption of constant friction is insufficient to describe reactions with complex reaction coordinates. In recent experiments, Höfer and coworkers investigated the fs-laser-induced diffusion of atomic oxygen on Pt(111).[56] Their measurements of the fluence dependence and the two-pulse correlation of the O hopping rate could only be reproduced if a temperature-dependent friction coefficient was assumed. The O-Pt motion is believed to be excited first and subsequently energy is transferred to the lateral, i.e., diffusive, motion via anharmonic coupling. Likewise, in current experiments in our laboratory on the fs-laser initiated $C+O \rightarrow CO$ formation reaction, the experimental data also suggest an electron temperature dependent friction $\eta_{el}=\eta_{el}(T_{el})$.[57] However, the origin of the breakdown of the 1D model is still unclear but intriguing.[53]

With this background and the results presented here for the $D_{ads}+D_{ads} \rightarrow D_{2,gas}$ reaction, theoretical frictional calculations extending the current model to higher dimensionality together with dynamical trajectory simulations will substantially help to differentiate ground from excited state effects (ground-state topology versus multidimensional nonadiabatic coupling to excited states). As a key reference system for these and other future investigations, the associative hydrogen desorption from Ru(0001) represents a prototype for a hot-electron driven surface reaction. Several comprehensive experiments have now provided quite a detailed microscopic understanding of various aspects of this reaction. Among these are the reaction mechanism and determining time constants,[10] the importance of adsorbate-adsorbate interactions[10,11] and finally the resulting energy proportions in different degrees of freedom as reported in this paper. Now theory is challenged by these experimental benchmarks to further reproduce and quantify the observed phenomena.

ACKNOWLEDGMENTS

We gratefully acknowledge J. Güdde and M. Luppi for sharing their work with us prior to publication. R. Dudek's help with the fs-laser system is appreciated. We also thank G. Ertl for his generous support. One of the authors (A.L.) wishes to thank the Alexander von Humboldt Stiftung for support during his stays in Berlin. In part, this work was funded by the Deutsche Forschungsgemeinschaft through Sfb450 and SPP1093.

*Electronic address: christian.frischkorn@physik.fu-berlin.de

[1] G. D. Kubiak, G. O. Sitz, and R. N. Zare, J. Chem. Phys. **83**, 2538 (1985).
[2] L. Schröter, R. David, and H. Zacharias, J. Electron Spectrosc. Relat. Phenom. **54-55**, 143 (1990).
[3] H. A. Michelsen, C. T. Rettner, and D. J. Auerbach, Phys. Rev. Lett. **69**, 2678 (1992).
[4] G. R. Darling and S. Holloway, Rep. Prog. Phys. **58**, 1595 (1995).
[5] A. Groß, Surf. Sci. Rep. **32**, 291 (1998).
[6] M. Bonn, A. W. Kleyn, and G. J. Kroes, Surf. Sci. **500**, 475 (2002).
[7] G. J. Kroes, A. Groß, E. J. Baerends, M. Scheffler, and D. A. McCormack, Acc. Chem. Res. **35**, 193 (2002).
[8] R. R. Cavanagh, D. S. King, J. C. Stephenson, and T. F. Heinz, J. Phys. Chem. **97**, 786 (1993).
[9] M. Bonn, S. Funk, C. Hess, D. N. Denzler, C. Stampfl, M. Scheffler, M. Wolf, and G. Ertl, Science **285**, 1042 (1999).
[10] D. N. Denzler, C. Frischkorn, C. Hess, M. Wolf, and G. Ertl, Phys. Rev. Lett. **91**, 226102 (2003).
[11] D. N. Denzler, C. Frischkorn, M. Wolf, and G. Ertl, J. Phys. Chem. B **108**, 14503 (2004).
[12] J. A. Prybyla, T. F. Heinz, J. A. Misewich, M. M. T. Loy, and J. H. Glownia, Phys. Rev. Lett. **64**, 1537 (1990).
[13] L. M. Struck, L. J. Richter, S. A. Buntin, R. R. Cavanagh, and J. C. Stephenson, Phys. Rev. Lett. **77**, 4576 (1996).
[14] G. Eichhorn, M. Richter, K. Al-Shamery, and H. Zacharias, Surf. Sci. **368**, 67 (1996).
[15] L. Cai, X. Xudong, and M. M. T. Loy, Surf. Sci. **464**, 727 (2000).
[16] T. Yamanaka, A. Hellman, S. Gao, and W. Ho, Surf. Sci. **514**, 404 (2002).
[17] C. Frischkorn, Surf. Sci. **593**, 67 (2005).
[18] K. D. Rendulic, G. Anger, and A. Winkler, Surf. Sci. **208**, 404 (1989).
[19] A. Groß, S. Wilke, and M. Scheffler, Phys. Rev. Lett. **75**, 2718 (1995).
[20] H. A. Michelsen and D. J. Auerbach, J. Chem. Phys. **94**, 7502 (1991).
[21] D. A. McCormack, G. J. Kroes, R. A. Olsen, J. A. Groeneveld, J. N. P. van Stralen, and E. J. B. R. C. Mowrey, Faraday Discuss. **117**, 109 (2000).
[22] B. Hammer, M. Scheffler, K. W. Jacobsen, and J. K. Nørskov, Phys. Rev. Lett. **73**, 1400 (1994).
[23] H. Eyring and M. Polanyi, Z. Phys. Chem. Abt. B **12**, 279 (1931).
[24] L. Diekenhöner, L. Hornekar, H. Mortensen, E. Jensen, A. Beurichter, and A. C. Luntz, J. Chem. Phys. **117**, 5018 (2002).
[25] P. Feulner and D. Menzel, Surf. Sci. **154**, 465 (1985).
[26] S. Funk, M. Bonn, D. N. Denzler, C. Hess, M. Wolf, and G. Ertl, J. Chem. Phys. **112**, 9888 (2000).
[27] D. Wetzig, M. Rutkowski, H. Zacharias, and A. Groß, Phys. Rev. B **63**, 205412 (2001).
[28] As an empirical function, the modified Maxwell-Boltzmann distribution $n_{\mathrm{flux}}(t)dt = At^{-5}\exp[-(m/2k_{\mathrm{B}}T)(d_0/t - v_0)^2]dt$ is frequently applied to reproduce a desorbing particle flux (see Refs. 30 and 31). A stands for a normalization constant including the solid angle and sensitivity of the detector, while d_0 is the flight distance. The introduction of the initial velocity v_0 allows more flexibility in the fitting routine. The entire distribution can be interpreted as a thermal distribution at temperature T superimposed on a stream velocity v_0 as produced, for instance, by a supersonic free jet expansion.
[29] G. Comsa and R. David, Surf. Sci. Rep. **5**, 145 (1985).
[30] F. M. Zimmermann and W. Ho, Surf. Sci. Rep. **22**, 127 (1995).
[31] E. Hasselbrink, *Laser Spectroscopy and Photochemistry on Metal Surfaces* (World Scientific, Singapore, 1995), p. 685.
[32] Note the factor of 2 due to the density-to-flux conversion of the raw experimental data recorded by a QMS (a density detector). In such a detector, slower particles have a higher ionization probability.
[33] S. I. Anisimov, B. L. Kapeliovich, and T. L. Perel'man, Sov. Phys. JETP **39**, 375 (1974).
[34] M. Brandbyge, P. Hedegard, T. F. Heinz, J. A. Misewich, and D. M. Newns, Phys. Rev. B **52**, 6042 (1995).
[35] The first digit refers to the vibrational quantum number of the resonantly excited state, whereas the second number specifies the vibrational quantum number of the initial, i.e., ground state. P and R denote the respective rotational branch and the last entry stands for the rotational quantum number of initial state.
[36] M. Rutkowski, D. Wetzig, H. Zacharias, and A. Groß, Phys. Rev. B **66**, 115405 (2002).
[37] C. H. Greene and R. N. Zare, Annu. Rev. Phys. Chem. **33**, 119 (1982).
[38] J. D. Lambert, *Vibrational and Rotational Relaxation in Gases* (Clarendon, Oxford, 1977).
[39] W. Meier, G. Ahlers, and H. Zacharias, J. Chem. Phys. **85**, 2599 (1986).
[40] H. Rabitz and S.-H. Lam, J. Chem. Phys. **63**, 3532 (1975).
[41] I. NoorBatcha, R. R. Lucchese, and Y. Zeiri, Phys. Rev. B **36**, 4978 (1987).
[42] J. P. Cowin, D. J. Auerbach, C. Becker, and L. Wharton, Surf. Sci. **78**, 545 (1978).
[43] The rotational *alignment* decay of the linear molecule C_2H_2 is significantly slower than the rotational *population* decay [see J. B. Halpern R. Dopheide, and H. Zacharias, J. Phys. Chem. **99**, 13611 (1995)]. Consequently, collisions between the desorbing D_2 in our experiment should also not affect the initial alignment of the molecules, which even have a smaller bond length than C_2H_2 and thus appear more spherical and less prone to alignment quenching interactions.
[44] Since the cross sections for translational-translational, translational-rotational, and translational-vibrational energy transfer relate as $\sigma_{\mathrm{TT}} \gg \sigma_{\mathrm{RT}} \gg \sigma_{\mathrm{VT}}$, a narrowing of the TOF spectra with increasing particle density, i.e., with higher laser fluence, would be expected if collisions played a crucial role after desorption.
[45] F. Budde, T. F. Heinz, A. Kalamarides, M. M. T. Loy, and J. A. Misewich, Surf. Sci. **283**, 143 (1993).
[46] In a reaction like the hydrogen recombination, which involves lateral approach of the reactants (diffusion), association, and desorption, the actual reaction coordinate should be in principle multidimensional. The success and limitations of a 1D model to describe such a system appropriately are discussed further below.
[47] K. W. Kolasinski, W. Nessler, A. de Meijere, and E. Hasselbrink, Phys. Rev. Lett. **72**, 1356 (1994).
[48] L. Schröter, H. Zacharias, and R. David, Phys. Rev. Lett. **62**, 571 (1989).
[49] J. C. Tully, Surf. Sci. **111**, 461 (1981).
[50] A. C. Luntz and M. Persson, J. Chem. Phys. **123**, 074704 (2005).

[51] J. K. Vincent, R. A. Olsen, G. J. Kroes, M. Luppi, and E. J. Baerends, J. Chem. Phys. **122**, 044701 (2005).
[52] M. Luppi, R. A. Olsen, and E. J. Baerends (unpublished).
[53] A. C. Luntz, M. Persson, S. Wagner, C. Frischkorn, and M. Wolf (unpublished).
[54] J. A. Misewich, T. F. Heinz, and D. M. Newns, Phys. Rev. Lett. **68**, 3737 (1992).
[55] The rotational overpopulation of states with $J'' < 6$ in the vibrational ground state of the desorbing D_2 molecules might be a consequence of the rotational cooling.
[56] K. Stépán, J. Güdde, and U. Höfer, Phys. Rev. Lett. **94**, 236103 (2005).
[57] S. Wagner, M. Krenz, A. Kaebe, M. Wolf, A. C. Luntz, and C. Frischkorn (unpublished).